

# Temporal variation in the winding number due to dynamical symmetry breaking and associated transport in a driven Su-Schrieffer-Heeger chain

Souvik Bandyopadhyay , Utso Bhattacharya, and Amit Dutta

*Department of Physics, Indian Institute of Technology, Kanpur, Kanpur 208016, India*



(Received 24 April 2019; revised manuscript received 26 June 2019; published 27 August 2019)

Considering a BDI symmetric one-dimensional Su-Schrieffer-Heeger model, we explore the fate of the bulk topological invariant, namely, the winding number under a generic time-dependent perturbation; the effective Hamiltonian, which generates the temporal evolution of the initial (ground) state of the completely symmetric initial Hamiltonian, may have the same or different symmetries. To exemplify, we consider the following protocols, namely (i) a perfectly periodic protocol, (ii) sudden changes in the parameters of the initial Hamiltonian. We establish that the topological invariant may change in some cases when the effective Hamiltonian (or the Floquet Hamiltonian in the periodic situation when observed stroboscopically) does not respect all BDI symmetries; this is manifested in the associated particle (polarization) or heat current in the bulk. Our results establish a strong connection between the time evolution of the winding number (thus, the associated transport of currents) and the symmetry of the Hamiltonian generating the time evolution, which has been illustrated considering an exhaustive set of possibilities. We also briefly dwell on the situation where the driving is not perfectly periodic.

DOI: [10.1103/PhysRevB.100.054305](https://doi.org/10.1103/PhysRevB.100.054305)

## I. INTRODUCTION

Recently, there has been an upsurge in the studies of topological condensed matter systems both from the theoretical [1–15] and experimental point of view [16–25] (for review see Refs. [26–30]). Symmetry protected topological phases of matter are characterized by gapped bulk states but with robust gapless excitations at the boundaries. Their novelty lies in the fact that they simply cannot be understood under the well-established Landau-Ginzburg paradigm, which classifies phases of matter distinguished by a local order parameter in terms of spontaneous symmetry breaking. Such phases of matter can only be characterized by global order parameters. For such noninteracting topological systems, the bulk-boundary correspondence serves as a guiding principle in decoding the phenomenology of topological insulators: Bulk topological invariants characterizing a given phase are uniquely reflected in gapless (metallic) boundary states. Therefore the bulk-boundary correspondence links a physically measurable quantity to a topological bulk invariant. In these systems, the topological invariant fundamentally distinguishes between the equivalence classes of all Hamiltonians respecting the same symmetry constraints. Two such Hamiltonians belonging to different equivalence classes but having the same symmetries cannot be adiabatically deformed into each other without closing the gap in the bulk spectrum (i.e., without crossing a gapless quantum critical point). Moreover in equilibrium, the boundary states are described by their own topological invariants, whose value must be equal to the invariant of the bulk insulator.

However, even in such systems symmetry considerations play a tremendous role. It has been possible to classify different topological phases of noninteracting systems [31] based on the constraints imposed on their Hamiltonians by

the symmetries they obey; attempts are being made to achieve a similar classification for interacting systems [32] and open quantum systems [33]. The lack of classification in terms of a local order parameter and the presence of a global (topological) order implies that the topological phases can be classified by determining certain bulk topological invariants such as the winding or the Chern number [27], which depend on the global character of the eigenvectors representing the system.

Experimental realizations of topological systems especially in cold atomic setups [34–38] have also opened up the possibility of subjecting them to time-dependent drives. These experimental studies have initiated a plethora of theoretical works on quenched and periodically driven topological systems [39–64]. This enables us to probe the robustness of the topological features of the ground states of such systems against time-dependent perturbations. Moreover, time-dependent drives that are periodic in time also leads to the realization of new topological phases of matter, which have no equilibrium counterpart [65–70].

Inspired by the above experimental studies, recently, the fate of topology in generic out of equilibrium systems are being extensively investigated in order to understand the nonequilibrium classification of topological systems [71–80]. Interestingly, it has been shown that for two-dimensional (2D) Chern insulating systems without boundaries, it is not possible to reach a nontrivial topological state via unitary evolution from a trivial initial state as the bulk Chern number remains invariant [71]. However, for the same systems with boundaries the edge states of such 2D systems can exhibit nontrivial dynamics as the bulk-boundary correspondence for such systems in its usual form does not hold out of equilibrium [72–74]. We note that the influence of nonequilibrium

dynamics on the equilibrium topology was also extensively studied in interacting topological Bardeen-Cooper-Schrieffer (BCS) superfluids with regard to two topological invariants defined with respect to the pseudospin configuration and the retarded nonequilibrium single-particle Green's function, respectively [81,82]. In these works it was shown that though the former invariant remains temporally invariant following a quench across a quantum critical point while the latter may change with time.

This brings us to the question that whether the out of equilibrium dynamics of one-dimensional (1D) topological systems also exhibit a behavior similar to the 2D situation. To address this question, we subject the paradigmatic topological 1D Su-Schrieffer-Heeger (SSH) model to time-dependent drives and investigate the following questions: (i) Is it possible to change the winding invariants of such a system under the application of a time-periodic drive? (ii) Do the symmetry constraints of the time-dependent perturbations affect the topological properties of the postquench states? Finally, (iii) What happens to the energy transport dynamics of such systems under the application of nonequilibrium perturbations such as sudden quenches?

In this work, we initially focus on a generically driven (with no *a priori* assumption of adiabaticity) SSH model in which we show that the bulk winding number characterizing the 1D system do vary in time only when the applied time-dependent perturbations break certain symmetries of the undriven Hamiltonian. This change of the winding number is also accompanied by the generation of an observable particle current; this attains a steady value, asymptotically in time, in the case of perfectly periodic driving. However, we further show that the presence of a biased random noise in the periodic drive results in the generation of an infinite temperature state, which is topologically featureless. In the noisy case, the accompanying particle current although settles to a prethermal region after exhibiting initial transient oscillations, but eventually decays to zero asymptotically with time in accordance with the infinite temperature behavior of the bulk invariant. Finally, we also focus on the possibility of local energy transport or heat current generation when the SSH system is subjected to sudden quenches. We show that the generation of heat currents in the system are related to different symmetry considerations of the applied time-dependent perturbations in comparison to the production of particle currents in the same system.

The paper is organized in the following fashion: In Sec. II A, we introduce the SSH model discussing the underlying topology and symmetry properties. The fate of the winding number in a generic driven system is discussed in Sec. III. The special situation of the periodic driving is discussed in Sec. IV where we show how the change in the winding number is manifested in the corresponding particle current generation in the bulk. Finally, in Sec. V, we identify the symmetries of the effective Hamiltonian that result in the heat current generation considering a sudden quenching protocol. In Appendix A, we address the situation when the driving is not perfectly periodic in time but is affected by biased random noisy perturbations and explore the fate of the polarization current.

## II. SU-SCHRIEFFER-HEEGER (SSH) MODEL

### A. Topological transition

The SSH model [27], which belongs to the BDI class of topological insulators is the simplest 1D model exhibiting an underlying topological structure and end states. Physically, it describes a 1D lattice with a two-atom sublattice structure in which the intralattice hopping amplitude is in general different from the interlattice hopping amplitude. The Hamiltonian for the SSH model can be written in terms of the (spin polarized) fermion creation and annihilation operators as,

$$H = \sum_{n=1}^{\mathcal{N}} (v c_{n,1}^\dagger c_{n,2} + w c_{n,2}^\dagger c_{n+1,1} + \text{H.c.}), \quad (1)$$

where H.c. denotes the Hermitian conjugate,  $v$  and  $w$  are the intracell and intercell hopping amplitudes, respectively, and  $\mathcal{N}$  is the total number of unit cells in the chain. The complex fermionic operator  $c_{n,i}^\dagger$  ( $c_{n,i}$ ) creates (destroys) a fermion in the sublattice position  $i$  ( $i = 1, 2$ ) of the  $n$ th unit cell and satisfies the fermionic anticommutation rules,

$$\{c_p^\dagger, c_q\} = \delta_{pq} \text{ and } \{c_p, c_q\} = \{c_p^\dagger, c_q^\dagger\} = 0. \quad (2)$$

After performing a tight-binding analysis one can write the Hamiltonian in Eq. (1) as,

$$H(k) = \bigoplus_k \vec{h}(k) \cdot \vec{\sigma}, \quad (3)$$

where,

$$\begin{aligned} h_x(k) &= \text{Re}(v) + |w| \cos(k + \arg(w)) \\ h_y(k) &= -\text{Im}(v) + |w| \sin(k + \arg(w)) \\ h_z(k) &= 0, \end{aligned} \quad (4)$$

where the lattice parameter is set equal to identity. This Hamiltonian has the following eigenvalue spectrum:

$$E(k) = \pm |\vec{h}(k)|, \quad (5)$$

and the respective eigenvectors are,

$$|\pm\rangle = \frac{1}{\sqrt{2}} \begin{pmatrix} \pm e^{-i\phi(k)} \\ 1 \end{pmatrix}, \quad (6)$$

where  $\phi = \tan^{-1}(\frac{h_y}{h_x})$ . It is clear from the Eq. (4), that  $\vec{h}(k)$  is periodic in  $k$  with a period of  $2\pi$ . Hence in the space of  $h_x$  and  $h_y$ ,  $\vec{h}(k)$  traces out a closed curve as  $k$  varies over the first Brillouin zone (in this case, a circle). Furthermore, the SSH model is classified through the following bulk topological winding number  $\nu$ , which is given as,

$$\nu = \frac{i}{2\pi} \int_{-\pi}^{\pi} dk \frac{d}{dk} \ln(h_x + ih_y) = \frac{i}{2\pi} \int_{\text{BZ}} \langle \psi_0^k | \partial_k | \psi_0^k \rangle dk, \quad (7)$$

which is quantized and can only assume integral values and is proportional to the change in the argument of  $\vec{h}(k)$  as  $k$  varies over the first Brillouin zone. Hence, if the circle in the parameter space does not enclose the origin,  $\nu$  is zero (i.e., if  $|v| > |w|$ ). On the other hand,  $\nu$  is one if the circle encloses the origin (i.e., if  $|v| < |w|$ ) and the chain hosts topologically protected robust end states. It is also evident from Eq. (5) that

the energy gap between the two bands vanishes at  $|v| = |w|$  and the winding number becomes undefined. Thus if the gap is not closed,  $\nu$  is well defined and is robust to external changes in the Hamiltonian and hence is a topological invariant clearly demarcating the topologically trivial and nontrivial phases.

### B. Symmetries

The topological classification of noninteracting many-body quantum systems are performed by considering three different discrete symmetries viz., the time-reversal symmetry ( $\mathcal{T}$ ), the particle-hole symmetry ( $\mathcal{P}$ ), and the sublattice (chiral) symmetry ( $\mathcal{S}$ ). The constraints imposed upon the Hamiltonian of a system possessing the above symmetries in the quasimomentum basis are expressed as,

$$\begin{aligned}\mathcal{T}^{-1}H(k)\mathcal{T} &= H(-k), \\ \mathcal{P}^{-1}H(k)\mathcal{P} &= -H(-k), \\ \mathcal{S}^{-1}H(k)\mathcal{S} &= -H(k),\end{aligned}\quad (8)$$

where  $\mathcal{T}$  and  $\mathcal{P}$  are antiunitary operators such that  $\mathcal{T}^2 = \pm\mathbb{I}$  and  $\mathcal{P}^2 = \pm\mathbb{I}$  whereas  $\mathcal{S}$  is an unitary operator satisfying where  $\mathcal{S}^2 = \mathbb{I}$  and  $\mathbb{I}$  is the  $2 \times 2$  identity operator. We also note that the sublattice symmetry is a combined effect of the time-reversal symmetry and the particle-hole symmetry as,

$$\mathcal{S} = \mathcal{T}\mathcal{P}. \quad (9)$$

It is now evident from the Hamiltonian of the SSH model in Eq. (3) and the symmetry transformations in Eq. (8) that the SSH model is symmetric under the sublattice transformation  $\mathcal{S} = \bigotimes_k \sigma_z$ , which results in the vanishing of  $h_z(k)$ . Also, if the hopping coefficients  $v$  and  $w$  are real, the Hamiltonian possesses time-reversal symmetry  $\mathcal{T} = \bigotimes_k \mathcal{K}$ ,  $\mathcal{K}$  being simply the complex conjugation operator. Hence, it is clear from Eq. (9) that the system is also symmetric under the particle-hole/charge conjugation operation with  $\mathcal{P} = \bigotimes_k \mathcal{K}\sigma_z$ . Therefore, as such the SSH model belongs to the BDI class of Hamiltonians within the topological classification scheme.

### III. THE FATE OF WINDING NUMBER FOLLOWING A GENERIC DRIVE

We consider the SSH model and study the temporal evolution of the equilibrium topological invariant, i.e., the winding number under a generic unitary drive. We begin with an initial state  $|\psi_k(0)\rangle$ , the system is allowed to evolve under the driven Hamiltonian  $H_k(t)$ . The state  $|\psi_k(0)\rangle$  therefore evolves with time as

$$\begin{aligned}|\psi_k(t)\rangle &= \mathbb{T} e^{-i \int_0^t H_k(t') dt'} |\psi_k(0)\rangle \equiv e^{-iH_k^{\text{eff}}(t)t} |\psi_k(0)\rangle \\ &= U_k(t) |\psi_k(0)\rangle,\end{aligned}\quad (10)$$

where  $H_k^{\text{eff}}(t)$  is the time-dependent effective Hamiltonian acting as a generator of the unitary evolution acting on the driven system and  $\mathbb{T}$  denotes the time ordering operator. We now investigate the fate of the winding number under such a time-dependent dynamics. To analyze this, let us recall the time-dependent or dynamical Berry connection as

$$A_k(t) \equiv [\langle \psi_k(0) | U_k^\dagger \partial_k U_k | \psi_k(0) \rangle], \quad (11)$$

which evolves in time as,

$$A_k(t) = \langle \psi_k(0) | \partial_k | \psi_k(0) \rangle + \langle \psi_k(0) | U_k^\dagger (\partial_k U_k) | \psi_k(0) \rangle$$

$$= A_k(0) + \langle \psi_k(0) | U_k^\dagger (\partial_k U_k) | \psi_k(0) \rangle. \quad (12)$$

Hence, the change in the Berry connection at a later time is given by,

$$\Delta A_k = A_k(t) - A_k(0) = \langle \psi_k(0) | U_k^\dagger (\partial_k U_k) | \psi_k(0) \rangle. \quad (13)$$

Recasting the effective Hamiltonian to the following form,  $H_k^{\text{eff}}(t) = |m(k, t)\rangle \langle \hat{m}(k, t) \cdot \vec{\sigma}$  and also denoting  $|m(k, t)\rangle$  simply as  $m$  we obtain,

$$\begin{aligned}U_k^\dagger (\partial_k U_k) &= \partial_k m \{ -it \sin^2 mt (\hat{m} \cdot \sigma) + i \sin^2 mt (\hat{m} \times \partial_k \hat{m}) \cdot \sigma \} \\ &\quad - i(\sin mt \cos mt) \partial_k \hat{m} \cdot \sigma.\end{aligned}\quad (14)$$

The initial state  $|\psi_k(0)\rangle$  that we consider happens to be the ground state of the SSH Hamiltonian (belonging BDI class), which can be chosen to be of the form of Eq. (6) where  $\phi(k)$  is an odd function of  $k$ . Interestingly, the terms on the right-hand side of the Eq. (14) can be shown to vanish individually when integrated over the entire Brillouin zone, pertaining to certain conditions imposed upon the effective Hamiltonian  $H_k^{\text{eff}}$  as discussed below.

Let us now analyze the implications of Eqs. (13) and (14). Taking the expectation value of the first term of the above equation with respect to the state  $|\psi_k(0)\rangle$ , one observes that the integral of this quantity over the full Brillouin zone vanishes identically if  $m_x(k)$  is an even function of  $k$  and  $m_y(k)$  is an odd function of  $k$ . Similarly, analyzing the integral of the next two terms over the full Brillouin zone, we see that both of them vanishes identically if  $m_z(k)$  is an odd function of  $k$  or zero in addition to the above constraints imposed on  $m_x(k)$  and  $m_y(k)$ . If the above conditions are satisfied by the effective Hamiltonian then the winding number must remain invariant in time.

It is evident from Eq. (8) that the above constraints on the single-particle Hamiltonian in  $k$  space, demand the presence of certain symmetries of the effective Hamiltonian. Namely, one concludes that the equilibrium winding number remains invariant under temporal evolution if the effective dynamical Hamiltonian ( $H_k^{\text{eff}}$ ) respects either of the symmetry combinations,  $\mathcal{T}$  and  $\mathcal{P}$  [ $m_x(k) \rightarrow \text{even}$ ,  $m_y(k) \rightarrow \text{odd}$ ,  $m_z(k) \rightarrow 0$ ] or just  $\mathcal{P}$  [ $m_x(k) \rightarrow \text{even}$ ,  $m_y(k) \rightarrow \text{odd}$ ,  $m_z(k) \rightarrow \text{odd}$ ].

### IV. PERIODIC DRIVING AND NONEQUILIBRIUM CURRENT GENERATION

#### A. Generic periodic driving

In this section, our focus is to look at an observable, which is the bulk polarization current density for various periodic driving protocols. It is straightforward to show [75] that in an arbitrary time-dependent situation the bulk polarization current density  $j(t)$  of the SSH chain is directly proportional to the rate of change of the topological winding number ( $\nu$ ):

$$j(t) = \frac{1}{2\pi} \int_{BZ} dk \langle \psi_k(t) | \partial_k H_k(t) | \psi_k(t) \rangle = \frac{d\nu}{dt}, \quad (15)$$

where  $|\psi_k(t)\rangle$  is the time-evolved state for each quasimomenta mode  $k$  and  $H_k(t)$  is the instantaneous time-dependent Hamiltonian. However, in the case of a time-periodic drive with a period  $T$ , the stroboscopic (measured after a complete period), the variation of the winding number denoted as  $\Delta \nu_m$  for the

$m$ th stroboscopic interval, is related to the average change in the bulk polarization density of the chain within the  $(m - 1)$ th and the  $m$ th period of evolution, i.e.,

$$\Delta v_m = \frac{v(mT) - v((m - 1)T)}{T} = \frac{1}{T} \int_{(m-1)T}^{mT} j(t) dt. \quad (16)$$

The average polarization over one time period if expanded shows a dependency on the symmetries of both the effective Hamiltonian [ $H_k^{\text{eff}}(t)$ ] and the instantaneous time-dependent Hamiltonian ( $H_k(t)$ ),

$$\begin{aligned} \Delta v_m &= \int_{(m-1)T}^{mT} \int_{BZ} dt dk \langle \psi_k(0) | e^{iH_k^{\text{eff}}(t)t} \\ &\times \partial_k H_k(t) e^{-iH_k^{\text{eff}}(t)t} | \psi_k(0) \rangle. \end{aligned} \quad (17)$$

Thus, if both  $H_k^{\text{eff}}(t)$  defined at every instant  $t$  but lying within the stroboscopic interval and the instantaneous  $H_k(t)$  preserve the above symmetries enlisted in Sec. III,  $\Delta v_m$  is zero at every instant of time  $t$ . Consequently the stroboscopic winding number  $v(mT)$  remains trivially invariant under the dynamics. Later we will see that the stroboscopic variation of the winding number completely depends on the symmetries respected by the Floquet Hamiltonian.

### B. Explicit symmetry breaking in a multistep periodic drive

In this section, we will be considering different kinds of periodic drives on a zero current carrying initial state of the SSH model, to probe whether after an asymptotically long time, the bulk polarization current density generated due to the change in the winding invariant attains a steady value when observed stroboscopically.

We consider a periodic drive with a two-step driving protocol applied within one stroboscopic time interval  $(0, T)$ ; on explicitly breaking certain symmetries in the Floquet Hamiltonian, the steady-state current attains a constant value starting from a zero current initial state. The bulk polarization current being an expectation value over the time-evolved state as defined in Eq. (15) reaches a periodic steady value asymptotically for large times [83]. Hence, when viewed stroboscopically, a constant steady current can be generated for large times in 1D topological systems by periodically driving provided that one dynamically breaks certain symmetries to be discussed in this section.

To achieve the symmetry breaking, we employ the two-step periodic drive, which involves the evolution of the initial state of the system under two piecewise continuous time-independent Hamiltonians viz.  $H_0(k)$  and  $H_1(k)$  in alternate time steps of width  $T/2$ , where the Hamiltonian  $H_0(k)$  is that of a BDI symmetric SSH model as in Eq. (3). Considering the Hamiltonians  $H_0(k) = \tilde{h}_0 \cdot \vec{\sigma}$  and  $H_1(k) = \tilde{h}_1 \cdot \vec{\sigma}$ , the effective propagator after the two time steps or after one complete period of driving therefore assumes the following form:

$$U_k(T) = e^{-iH_1(k)\frac{T}{2}} e^{-iH_0(k)\frac{T}{2}}. \quad (18)$$

The above propagator  $U_k(T)$  may be expanded using Euler's identity as,

$$U_k(T) = \alpha(k, T)\mathbb{1} - i\tilde{m}(k, T) \cdot \vec{\sigma}, \quad (19)$$

where,

$$\alpha(k, T) = \cos \frac{h_1 T}{2} \cos \frac{h_0 T}{2} - \sin \frac{h_1 T}{2} \sin \frac{h_0 T}{2} (\hat{h}_1 \cdot \hat{h}_0)$$

and

$$\begin{aligned} \tilde{n}(k, T) &= \cos \frac{h_1 T}{2} \sin \frac{h_0 T}{2} \hat{h}_0 + \sin \frac{h_1 T}{2} \cos \frac{h_0 T}{2} \hat{h}_1 \\ &+ \sin \frac{h_1 T}{2} \sin \frac{h_0 T}{2} (\hat{h}_1 \times \hat{h}_0). \end{aligned} \quad (20)$$

The stroboscopic (over a complete period) evolution operator can be written in the form,

$$\begin{aligned} U_k(T) &= \mathbb{T} e^{-i \int_0^T H_k(t') dt'} = e^{-iH_F(k)T} \\ &= \cos(m_F T)\mathbb{1} - i \sin(m_F T)(\hat{m}_F \cdot \vec{\sigma}), \end{aligned} \quad (21)$$

where  $H_F = \vec{m}_F \cdot \vec{\sigma}$  is the Floquet Hamiltonian and  $\mathbb{T}$  is the time-ordering operator.

Comparing Eq. (19) and Eq. (21), one obtains,

$$\begin{aligned} \cos(m_F T) &= \alpha(k, T) \\ \sin(m_F T)m_{F,i} &= n_i(k, T), \end{aligned} \quad (22)$$

where,  $m_F = |\vec{m}_F|$  and  $i = 1, 2, 3$  represents the components of the three Pauli matrices in Eq. (19). It is thus sufficient to identify the symmetries respected by the term  $\beta(k, T) = \tilde{n}(k, T) \cdot \vec{\sigma}$  in Eq. (19) to uncover the symmetries of Floquet Hamiltonian  $H_F(k)$ . One therefore identifies the symmetries respected by  $\beta(k, T)$  and its dependence on the symmetries respected by the individual step Hamiltonians  $H_0(k)$  and  $H_1(k)$  in accordance with Eq. (8) to understand stroboscopic dynamics.

Starting from the eigenstate of a completely  $\mathcal{T}$ ,  $\mathcal{P}$ , and  $\mathcal{S}$  symmetric SSH model and using Eq. (13), the stroboscopic change in the winding number is observed to depend only on the symmetries of the Floquet Hamiltonian, i.e.,

$$v(mT) = v(0) + \frac{i}{2\pi} \oint \langle \psi_k(mT) | (\partial_k e^{-iH_F(k)mT}) | \psi_k(0) \rangle dk. \quad (23)$$

We therefore conclude that it is the symmetry of  $H_F$  that completely determines the stroboscopic variation of the winding number and the stroboscopic polarization current defined by

$$J(NT) = \frac{1}{2\pi} \int_{BZ} \langle \psi_k(NT) | \partial_k H_0(k) | \psi_k(NT) \rangle. \quad (24)$$

Arguing in similar lines to Sec. III, it is straightforward to show that the stroboscopic winding number remains dynamically invariant if the Floquet Hamiltonian  $H_F(k)$  respects either  $\mathcal{P}$  symmetry or both  $\mathcal{P}$  and  $\mathcal{T}$  symmetries and the stroboscopic polarization current vanishes.

First, we focus on an interesting situation in which the stroboscopic winding number remains invariant despite the explicit breaking of  $\mathcal{P}$  symmetry in the instantaneous Hamiltonian  $H_k(t)$  and the effective Hamiltonian  $H_k^{\text{eff}}(t)$ . If the Floquet Hamiltonian defined in Eq. (21), preserves the identified symmetries while the effective Hamiltonian and the time-dependent Hamiltonian breaks the symmetries explicitly within the time interval, the winding number is seen to remain invariant stroboscopically but not within the time period of the drive.

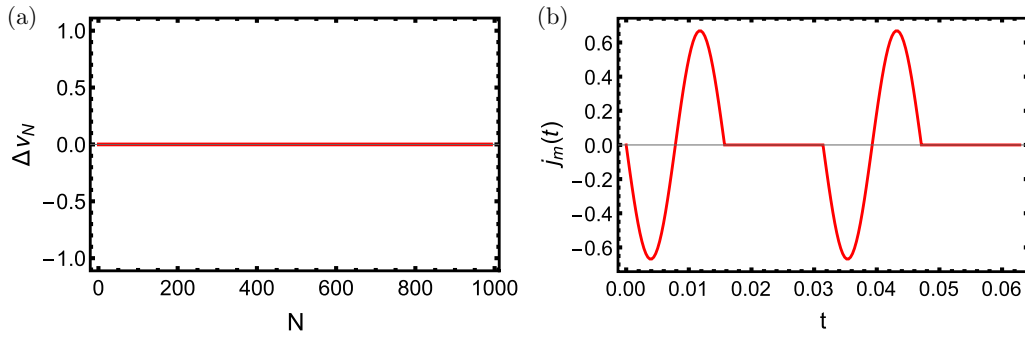


FIG. 1. (a) Stroboscopic change in winding number under a periodic drive that breaks the  $\mathcal{P}$  symmetry in the time varying Hamiltonian  $H_k(t)$  [as defined in Eq. (25)] and the effective Hamiltonian  $H_k^{\text{eff}}$  while preserving all BDI symmetries in the Floquet Hamiltonian, which is a BDI SSH chain [as discussed after Eq. (26)], with the hopping parameters  $v = 0.6$  and  $w = 0.8$  for a system size of  $L = 1000$  and  $\omega = 2\pi/T = 100$ . (b) Particle current generation in micromotion within a time interval  $(0, T)$  under a periodic drive breaking  $\mathcal{P}$  symmetry in the time varying Hamiltonian  $H_k(t)$  and the effective Hamiltonian  $H_k^{\text{eff}}$  [as in Eq. (25)] the corresponding Floquet Hamiltonian is again a BDI SSH chain with the hopping parameters  $v = 0.6$  and  $w = 0.8$  for a system size of  $L = 1000$  and  $\omega = 100$ . We observe that although there is an instantaneous polarization current, the same when averaged over a complete period vanishes. These cases are discussed in Sec. IV B.

The polarization current generated in such situations is nonzero only in the dynamics of the system within a complete period of the drive. The bulk polarization current  $j_m(t)$  generated within the  $m$ th periodic interval is given by (15) with  $t \in [(m-1)T, mT]$ . However, this current generated in the micromotion of the system when averaged over the complete period of the drive vanishes to keep the stroboscopic winding number dynamically invariant. Therefore, although an instantaneous polarization current gets generated but when averaged over a complete period, the total change in the bulk polarization over a complete period is zero. We illustrate the particular situation by considering a specific drive that breaks the  $\mathcal{P}$  symmetry in the instantaneous Hamiltonian  $H_k(t)$  while preserving the  $\mathcal{T}$  symmetry,

$$\begin{aligned} H_k(t) &= H_1(k), & \text{for } 0 \leq t \leq \frac{T}{4}, \\ H_k(t) &= M\sigma_z, & \text{for } \frac{T}{4} \leq t \leq \frac{T}{2}, \\ H_k(t) &= H_2(k), & \text{for } \frac{T}{2} \leq t \leq \frac{3T}{4}, \\ H_k(t) &= H_0(k), & \text{for } \frac{3T}{4} \leq t \leq T, \end{aligned} \quad (25)$$

where  $H_0(k)$  is a BDI symmetric SSH Hamiltonian as stated in Eq. (3). The Hamiltonians  $H_1(k)$  and  $H_2(k)$  do not respect  $\mathcal{P}$  symmetry while preserving  $\mathcal{T}$  symmetry,

$$H_{1,2}(k) = \pm H_0(k) \pm M\sigma_z. \quad (26)$$

Using the identities in Eq. (22) repetitively to the Hamiltonian defined in Eq. (25), it is straightforward to show that the effective Hamiltonian  $H_k^{\text{eff}}(t)$  [see Eq. (10)] breaks all the BDI symmetries explicitly. However, when  $M = 2\omega$  with  $\omega = 2\pi/T$ , the Floquet Hamiltonian over the complete period reduces to simply the BDI symmetric SSH model described by  $H_0(k)$ . This completely BDI symmetric form of  $H_F(k)$  guarantees the invariance of the stroboscopic winding number in such cases and thus the polarization current averaged over a complete period vanishes [see Fig. 1(a) and Fig. 1(b)].

We hereafter proceed to discuss the different physical situations in which the BDI symmetries may be broken in the Floquet Hamiltonian [by tuning the symmetries of the step Hamiltonian  $H_1(k)$ ] to generate a stroboscopic polarization current.

### C. Breaking $\mathcal{P}$ and $\mathcal{S}$ while preserving $\mathcal{T}$ in $H_1(k)$

The breaking of the  $\mathcal{P}$  symmetry in  $H_1(k)$  of Eq. (18) can be achieved in a variety of ways which we illustrate below: (i) by introducing a real staggered next-nearest-neighbor hopping ( $B_1$ ) and (ii) by adding a staggered on-site potential ( $B_2$ ). Referring to (4), the Hamiltonian  $H_1(k)$  occurring in Eq. (18) for these situations are as follows.

( $B_1$ ) Staggered NNN hopping:

$$H_1(k) = (v + w \cos k)\sigma_x + w \sin k\sigma_y + f \cos k\sigma_z. \quad (27)$$

( $B_2$ ) Staggered on-site potential:

$$H_1(k) = (v + w \cos k)\sigma_x + w \sin k\sigma_y + M\sigma_z. \quad (28)$$

The bulk polarization current defined in Eq. (15) in the situations  $B_1$  and  $B_2$  reaches a steady value starting from zero; this is shown in Fig. 2(a) and Fig. 2(b), respectively. In both the cases however, the time-reversal symmetry remains preserved in  $H_1(k)$ .

### D. Breaking $\mathcal{P}$ and $\mathcal{T}$ but preserving $\mathcal{S}$ in $H_1(k)$

We now break the  $\mathcal{T}$  and  $\mathcal{P}$  symmetry together in  $H_1(k)$ , by making the intercell hopping amplitude  $w$  to be completely imaginary in  $H_1(k)$  in Eq. (18). This, however, preserves the chiral symmetry ( $\mathcal{S}$ ) resulting in,

$$H_1(k) = (v - w \sin k)\sigma_x + w \cos k\sigma_y. \quad (29)$$

The bulk polarization current defined in Eq. (15) in this scenario also reaches a steady value starting from zero as can be observed from Fig. 3(a).

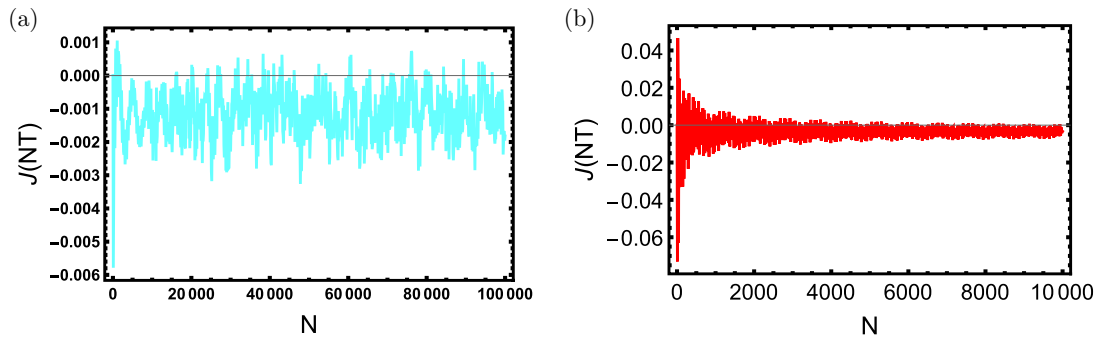


FIG. 2. (a) Stroboscopic particle current in a periodically driven SSH chain, breaking  $\mathcal{P}$  symmetry by introducing a real NNN hopping in  $H_1(k)$  [as discussed in Eq. (27) of the Sec. IV C] while preserving  $\mathcal{T}$  in  $H_1(k)$ . The initial and final hopping strengths are chosen to be  $v = 2.5$ ,  $w = 1.5$ , and a NNN hopping strength of  $f = 1.0$  for a system size  $L = 500$ ; the frequency of the periodic drive being  $\omega = 100$ . (b) Stroboscopic particle current in a periodically driven SSH chain, breaking  $\mathcal{P}$  by introducing a staggered mass in  $H_1(k)$  [Eq. (28) discussed in Sec. IV C] while preserving  $\mathcal{T}$  in  $H_1(k)$ . The initial and final hopping strengths are chosen to be  $v = 0.2$ ,  $w = 1.5$ , and a staggered mass of  $M = 1.0$  for a system size  $L = 1000$ , and  $\omega = 100$ .

### E. Breaking $\mathcal{P}$ , $\mathcal{T}$ , and $\mathcal{S}$ in $H_1(k)$

Furthermore, the breaking of all the three symmetries  $\mathcal{P}$ ,  $\mathcal{T}$ , and  $\mathcal{S}$  in  $H_1(k)$  can simply be achieved by selecting,

$$H_1(k) = (v - w \sin k)\sigma_x + w \cos k \sigma_y + M \sigma_z, \quad (30)$$

where  $M$  is a constant quasimomenta independent mass term. The bulk polarization current once again attains a steady nonzero value as can be seen in Fig. 3(b).

However, from Eq. (22) it must be noted that all the BDI symmetries have been broken in the resulting Floquet Hamiltonian  $H_F(k)$  in the scenarios considered in Secs. IV C, D, and E. The lack of the particle-hole symmetry in the Floquet Hamiltonian leads to the generation of a steady bulk polarization current.

## V. HEAT CURRENT GENERATION THROUGH DYNAMICAL SYMMETRY BREAKING THROUGH A SUDDEN QUENCH

The dynamical breaking of symmetries in the SSH model is also accompanied by a nonequilibrium energy flow in the bulk, which we analyze in this section. To analytically study the local energy current we resort to a local energy operator

defined in the bulk [84]. It changes in time according to the continuity equation expressed in terms of the divergence of the heat current operator. In all the cases discussed below, the initial Hamiltonian is the BDI SSH model in Eq. (1). We are suddenly changing the parameters of the Hamiltonian (or including a staggered on-site potential) to a final Hamiltonian  $\mathcal{H}$ , which may or may not respect the symmetries of the initial Hamiltonian.

The first situation we consider is that the final postquench Hamiltonian  $\mathcal{H}$  does not have a on-site potential and respects the time-reversal symmetry ( $\mathcal{T}$ ) and particle-hole symmetry ( $\mathcal{P}$ ) as given in Eq. (1) can be written as,

$$\mathcal{H} = \sum_i E_{i,i+1}, \quad (31)$$

where the term  $E_{i,i+1}$  connects the  $i$ th site with the  $(i+1)$ th site and the summation extends over the chain length assuming a periodic boundary conditions. The local energy current in the Heisenberg picture can then be written in terms of a continuity equation,

$$\frac{\partial E_{i,i+1}^h(t)}{\partial t} = -i[\mathcal{H}, E_{i,i+1}^h(t)] = -[j_{i+1}^h(t) - j_i^h(t)], \quad (32)$$

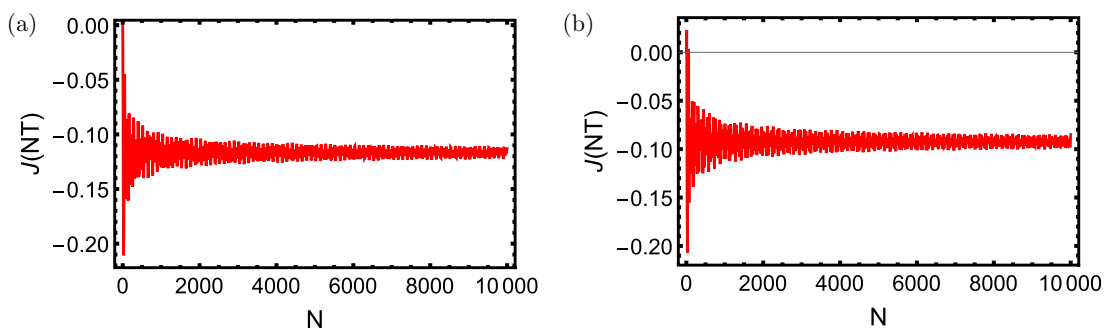


FIG. 3. (a) Stroboscopic particle current in a periodically driven SSH chain, breaking  $\mathcal{P}$  and  $\mathcal{T}$  by introducing an imaginary intercell hopping in  $H_1(k)$  but preserving  $\mathcal{S}$  [see Eq. (29) in Sec. IV D]. The initial and final hopping strengths are chosen to be  $v = 0.2$ ,  $w = 1.5i$  for a system size  $L = 1000$ , with  $\omega = 100$ . (b) Stroboscopic particle current in a periodically driven SSH chain, breaking  $\mathcal{P}$ ,  $\mathcal{T}$ , and  $\mathcal{S}$  in  $H_1(k)$  by introducing a staggered mass and an imaginary intercell hopping in  $H_1(k)$  [Eq. (30) in Sec. IV E]. The initial and final hopping strengths are chosen to be  $v = 0.2$ ,  $w = 1.5$  and a staggered mass of  $M = 1.0$  for a system size  $L = 1000$ ,  $\omega = 100$ .

where the superscripts  $h$  imply that the corresponding operators are written in the Heisenberg picture, which we shall omit in the subsequent discussion. The last equality enforces the conservation of energy thereby defining the local energy current operator  $J_i^E$ , where the superscript implies the heat current. Given the form of the Hamiltonian Eq. (31), it is straightforward to show that the heat current operator assumes the form,

$$j_i^E = -i[E_{i-1,i}, E_{i,i+1}]. \quad (33)$$

Comparing with the SSH Hamiltonian Eq. (1) and recasting it to a modified form,

$$\begin{aligned} \mathcal{H} &= \sum_i (vc_{2i-1}^\dagger c_{2i} + wc_{2i}^\dagger c_{2i+1} + \text{H.c.}) \\ &= \sum_i (E_{2i-1,2i} + E_{2i,2i+1}), \end{aligned} \quad (34)$$

where the odd sites reside on the A sublattice and the even sites reside on the B sublattice. The total energy current operator can then be formulated by summing over all the even and odd sites of the chain and using the anticommutation relations in Eq. (2),

$$\begin{aligned} J^E &= -i \sum_i vw(c_{2i-2}^\dagger c_{2i} + c_{2i-1}^\dagger c_{2i+1}) \\ &\quad + v^*w^*(c_{2i-2}c_{2i}^\dagger + c_{2i-1}c_{2i+1}^\dagger). \end{aligned} \quad (35)$$

Now, utilizing the translational invariance of the periodically wrapped chain, one can rewrite the energy current operator in Fourier space explicitly reintroducing the sublattice index (A or B),

$$J^E = \sum_k (c_{kA}^\dagger \ c_{kB}^\dagger) j_k^E \begin{pmatrix} c_{kA} \\ c_{kB} \end{pmatrix}, \quad (36)$$

where  $j_k^E$  is a  $2 \times 2$  matrix,

$$j_k^E = -i(vwe^{-ik} - v^*w^*e^{ik})\mathbb{I}, \quad (37)$$

$\mathbb{I}$  being a  $2 \times 2$  identity matrix. The total energy current in a state  $|\psi_k\rangle$  is then obtained by integrating the expectation value of  $J_k^E$  over the complete Brillouin zone,

$$J_\psi^E = \int_{\text{BZ}} dk \langle \psi_k | J_k^E | \psi_k \rangle, \quad (38)$$

which in the SSH model sums up to,

$$J_\psi^E = 2 \int_{-\pi}^{\pi} dk \text{Im}(vwe^{-ik}). \quad (39)$$

It is important to note that the energy current operator  $J_k^E$  is a multiple of identity and hence, commutes with the Hamiltonian [as is clear from Eq. (37)]. This causes  $J_\psi^E$  to remain invariant in time. Utilising the above analytical framework, we study the behavior of the heat current in the light of different symmetries of the evolving Hamiltonian following a sudden quench.

### A. Preserving both $\mathcal{P}$ and $\mathcal{T}$

We consider a sudden quench of the hopping strengths from an initial value of  $v$  and  $w$  to  $v'$  and  $w'$ , respectively,

such that it preserves both the symmetries ( $\mathcal{P}$  and  $\mathcal{T}$ ) in the final Hamiltonian [refer to Eq. (1)]. For the total bulk energy current, one obtains the expression,

$$J_\psi^E = 2v'w' \int_{-\pi}^{\pi} dk \sin k = 0. \quad (40)$$

Also, since the energy current is a conserved quantity in this case, it remains zero throughout the time evolution.

### B. Breaking both $\mathcal{P}$ and $\mathcal{T}$

When the intersublattice hopping parameter, i.e.,  $w$  is suddenly changed to a complex value in the final evolving Hamiltonian both  $\mathcal{P}$  and  $\mathcal{T}$  are broken. From the expression for the energy current in Eq. (39), it is straightforward to show that the current operator still remains a multiple of  $\mathbb{I}$  resulting in

$$J_\psi^E = 2v'w' \int_{-\pi}^{\pi} dk \cos k = 0. \quad (41)$$

Hence in this case as well, the bulk heat current vanishes for all times. This is to be contrasted to the case of a surviving time-dependent particle current as has been illustrated in Fig. 3(a).

### C. Breaking $\mathcal{P}$ while preserving $\mathcal{T}$

In this protocol, a staggered on-site potential is suddenly introduced in the free SSH chain; this breaks  $\mathcal{P}$  while preserving  $\mathcal{T}$  as has been shown in Eq. (28). Due to the breaking of the particle-hole symmetry, the final Hamiltonian assumes the following form:

$$\mathcal{H}_\mathcal{T} = H_{SSH} + \sum_i M c_{2i}^\dagger c_{2i} - M c_{2i-1}^\dagger c_{2i-1}, \quad (42)$$

where  $H_{SSH}$  is the bare and symmetric Hamiltonian of the periodically wrapped SSH chain (34). In the presence of the on-site potential, however, the expression of the local energy current must be rewritten to incorporate the additional diagonal terms in the Hamiltonian. Proceeding in similar lines as to the derivation of the Eq. (33), one obtains,

$$j_i^E = -i([E_{i-1,i}, E_{i,i+1}] + [E_{i-1,i}, E_{i,i}]), \quad (43)$$

where  $E_{i,i}$  are the symmetry-breaking diagonal terms of the Hamiltonian  $H_\mathcal{T}$ . Simplifying the above expression using the postquench Hamiltonian  $H_\mathcal{T}$ , the fermion anticommutation relations and the translational invariance of the chain, the local current operator is expressed in the momentum space as,

$$J_k^E = \vec{j}_i^E(k) \cdot \vec{\sigma}, \quad (44)$$

where,

$$\begin{aligned} j_0^E(k) &= 2 \text{Im}(vwe^{-ik}) \\ j_x^E(k) &= Mw \sin k \\ j_y^E(k) &= M(v + w \sin k) \\ j_z^E(k) &= 0. \end{aligned} \quad (45)$$

Interestingly, it is observed that apart from the contribution proportional to the identity matrix [as in Eq. (37)], nontrivial

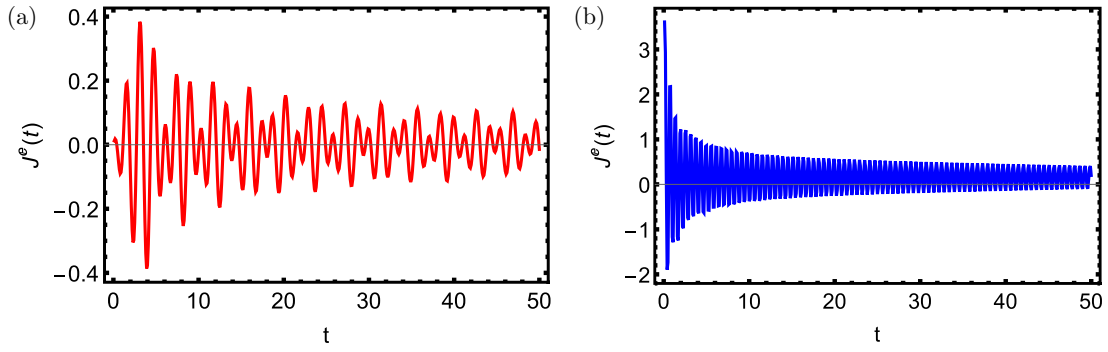


FIG. 4. (a) Heat current generation in the bulk in a quenched SSH chain by breaking  $\mathcal{P}$  through the sudden introduction of a staggered mass, which preserves  $\mathcal{T}$  in the final quenched Hamiltonian  $\mathcal{H}_{\mathcal{T}}$  [Eq. (42) in Sec. V C]. The initial and final hopping strengths are chosen to be  $v = 0.5$ ,  $w = 1.5$ , and a staggered mass in  $\mathcal{H}_{\mathcal{T}}(k)$  of  $M = 1.0$  with  $L = 500$ . (b) Heat current generation in the bulk in a quenched SSH chain by breaking  $\mathcal{T}$  through the sudden introduction of an imaginary staggered NNN hopping in  $\mathcal{H}_{\mathcal{P}}(k)$  while preserving  $\mathcal{P}$  in the final quenched Hamiltonian [as discussed in Eq. (48) in Sec. V D]. The initial and final hopping strengths are chosen to be  $v = 0.5$ ,  $w = 1.5$ , and a NNN hopping strength of  $f = 5.0i$  in  $\mathcal{H}(k)$  and  $L = 500$ .

nondiagonal terms have appeared in the local heat current operator in the presence of the staggered on-site potential.

Using the above components to evaluate the total heat current according to Eq. (38), one obtains the following analytic expression for the heat current,

$$J^E(t) = M \int_{-\pi}^{\pi} dk \frac{\sin(2m_f t)}{m_f} [j_y^E(k) \cos \phi - j_x^E(k) \sin \phi], \quad (46)$$

where  $H_{\mathcal{T}}(k) = \tilde{m}^f(k) \cdot \vec{\sigma}$ ,  $m_f = |\tilde{m}_f(k)|$ ,  $H_{SSH}(k) = \tilde{m}^i(k) \cdot \vec{\sigma}$ , and  $\phi = \tan^{-1} \left[ \frac{m_y^f(k)}{m_x^f(k)} \right]$ . Thus, the SSH model now shows nonzero flow of heat [see Fig. 4(a)] in the bulk as a consequence of the dynamical breaking of  $\mathcal{P}$  symmetry while the  $\mathcal{T}$  symmetry remains intact.

#### D. Breaking $\mathcal{T}$ while preserving $\mathcal{P}$

It is also possible to break the  $\mathcal{T}$  symmetry of the SSH model while keeping the  $\mathcal{P}$  symmetry intact by suddenly switching on a complex staggered next-nearest-neighbor hopping term, which renders the single-particle final Hamiltonian  $H_{\mathcal{P}}(k)$  to be of the form,  $H_{\mathcal{P}}(k) = \tilde{m}^f(k) \cdot \vec{\sigma}$  such that  $(m_x^f, m_y^f, m_z^f)$  are (even, odd, odd) functions of  $k$ , respectively. Now,

$$\mathcal{H}_{\mathcal{P}} = H_{SSH} + \sum_i (f c_{2i}^\dagger c_{2i+2} + f c_{2i-1}^\dagger c_{2i+1} + \text{H.c.}). \quad (47)$$

Setting the next-nearest hopping strength to be complex,  $f = \lambda i$  where  $\lambda \in \mathbb{R}$  yields the final Hamiltonian,

$$\mathcal{H}_{\mathcal{P}}(k) = (v + w \cos k) \sigma_x + w \sin k \sigma_y + \lambda \sin k \sigma_z. \quad (48)$$

This clearly shows that the  $\mathcal{T}$  symmetry has been broken in the system while keeping  $\mathcal{P}$  preserved throughout. As a result, the energy current, however, will now have two contributions, one from the nearest-neighbor hopping and the other from the next-nearest-neighbor hopping originating from the same site, i.e.,

$$j^E(k) = \sum j^{(1)}(k)_A + j^{(1)}(k)_B + \sum j^{(2)}(k)_A + j^{(2)}(k)_B, \quad (49)$$

where the summation extends over all the lattice sites.  $j^{(1)}(k)$  are the nearest-neighbor current and  $j^{(2)}(k)$  are the next-nearest-neighbor current. Expressing the total heat current operator in the  $2 \times 2$  sublattice basis as Eq. (44), one obtains,

$$\begin{aligned} j_0^E(k) &= 2 \text{Im}(v w e^{-ik} - \lambda^2 e^{-2ik}) \\ j_x^E(k) &= -\lambda(w - v \cos k) \\ j_y^E(k) &= -\lambda(v \sin k) \\ j_z^E(k) &= 0, \end{aligned} \quad (50)$$

which is nonzero when integrated over the complete Brillouin zone [Fig. 4(b)]. Thus, we see that the heat current in such a situation is nonzero although the particle current vanishes when  $\mathcal{P}$  is preserved by the final Hamiltonian.

## VI. CONCLUSIONS

In this work, we have studied the particle and heat transport properties of a time-dependent 1D topological quantum system. The goal is to test the robustness of the 1D topological phase against the inclusion of dynamical perturbations and the possible change in the associated winding number. Therefore, we resort to the simple 1D SSH model, to investigate the effect on the transport, namely the polarization current and the heat current, in such systems when the symmetries of the underlying system may be broken by the time-dependent perturbations. We focus on the issue whether the winding number can be changed through out of equilibrium drives and whether such a change can be captured in the transport properties of the system. In our work, the time evolution of the initial state of the 1D system is introduced through time-periodic drives, quantum quenches, and noisy perturbations that break the perfect time periodicity. We see that through the dynamical breaking of certain discrete (noncrystal) symmetries namely the particle-hole ( $\mathcal{P}$ ), time-reversal ( $\mathcal{T}$ ), and the chiral symmetry ( $\mathcal{S}$ ), there can be a generation of either particle or heat current in the bulk of the 1D chain accompanied by a change in the winding invariant with time.

Specifically in the periodic situation, we observe the following behavior: (i) When only the particle-hole symmetry is

broken in the instantaneous Hamiltonian or within the period of a drive, particle current is generated. However, the breaking of this  $\mathcal{P}$  in the instantaneous Hamiltonian does not guarantee that the bulk Floquet Hamiltonian, which governs the dynamics of the system at stroboscopic intervals, will also have a broken  $\mathcal{P}$  symmetry. Nonetheless, if the  $\mathcal{P}$  symmetry still remains preserved in the Floquet Hamiltonian, the winding number will still be conserved when observed stroboscopically. (ii) When the Floquet Hamiltonian also breaks the  $\mathcal{P}$  symmetry, we see the stroboscopic generation of a particle current in the system even when the initial state carried zero current. (iii) The generated current in case (ii) Following some initial transients eventually settles down to a steady nonzero value asymptotically in time.

One may wonder what happens when the system is subjected to biased random noisy perturbations that break the perfect periodicity of the drive. Interestingly, as we have illustrated in Appendix A, when the perfect time periodicity within a period is broken due to the presence of such perturbations, the particle current although shows a significant prethermal value, eventually decays to zero asymptotically with time reflecting the fact that the system reaches an infinite temperature ensemble. We note that this happens even when both the drive and the noisy perturbations break the  $\mathcal{P}$  symmetry explicitly.

Finally, we also probe the out of equilibrium behavior of the energy transport in the bulk of the system due to time-dependent driving in the form of sudden quenches. We observe that even when there is no heat current flowing in the system initially, dynamical breaking of either  $\mathcal{P}$  or  $\mathcal{T}$ , but not both, results in the generation of a heat current in the bulk of the system. This is notably different in comparison to the dynamical conditions that result in the flow of a particle current in the system. The notably different behavior of the particle and the energy current with respect to the symmetries of the drive is an artefact of nonequilibrium dynamics. As in out of equilibrium situations, the instantaneous state of the system does not necessarily respect the same set of symmetries as that of the instantaneous Hamiltonian, a complete physical understanding of the dynamics is an interesting direction of further research.

As mentioned previously in Sec. I, the Chern number stays temporally invariant under unitary dynamics and hence the unitary preparation of Floquet Chern insulators is difficult to achieve. Unlike the Chern number, we have observed that the winding number may change under unitary dynamics and hence it may be possible to dynamically engineer 1D topological phases with a nontrivial winding number through unitary driving protocols.

Recently discrete-time quantum walks have been shown to simulate all known topological phases in one and two dimensions [85–87]. A discrete time quantum walk can be viewed as a stroboscopic simulation of time evolution by an effective Hamiltonian. In our work, we are, however, considering the application of a periodic drive to a one-dimensional model and probing the possible temporal variation of the winding number. Whether these two approaches are related is an interesting question, which requires further studies.

The polarization current as well as the energy current flowing through the bulk of the chain being observables can be experimentally measured in a transport set up and hence the

predictions made in this work can be verified. We recall that in the process of an adiabatic quantum pump characterized by the topology of the pumping cycle, the dynamical state of the system follows the adiabatically evolving Hamiltonian. Therefore, the conclusions reached through our work regarding the symmetries of the Floquet Hamiltonian, would naturally manifest in the topological transport of charge across a SSH chain under an adiabatic periodic perturbation.

## ACKNOWLEDGMENTS

We acknowledge Sourav Bhattacharjee, S. Laha, and S. Maity for discussions. S.B. acknowledges CSIR, India for financial support.

## APPENDIX: BULK TOPOLOGICAL INVARIANT IN AN APERIODICALLY DRIVEN SYSTEM

We consider two 1D SSH Hamiltonians, one in the BDI class, i.e., respecting both time-reversal and particle-hole symmetries whereas the other breaks either or both of the symmetries  $\mathcal{P}$  and  $\mathcal{T}$  along with  $\mathcal{P}$ . Thus, under the first Hamiltonian  $H_0(k)$  the winding number remains invariant in time, whereas under the second Hamiltonian  $H_1(k)$  the winding number does not. The system is then subjected to an imperfect drive with an inherent probabilistic evolution where at each time step of width  $T/2$  the dynamical Hamiltonian is chosen randomly between  $H_0(k)$  and  $H_1(k)$ . The choice between  $H_0(k)$  and  $H_1(k)$  depends on the value of a random variable following a binomial distribution with a bias  $p$ . In the context of thermalization, such a random driving protocol have been studied in Refs. [88–90].

Introducing aperiodicity in the driving protocol, renders the system dynamically nonintegrable. Under an aperiodic drive, observing the dynamics stroboscopically at intervals of  $T$  modifies the relation established in Eq. (16) connecting the nonequilibrium stroboscopic current density and the temporal evolution of the bulk topological index. The current density when averaged over all disorder configurations and over a complete period  $T$  results in,

$$\frac{1}{T} \int_{(m-1)T}^{mT} dt \overline{j(t)} = \frac{1}{T} [\overline{v(mT)} - \overline{v((m-1)T)}], \quad (\text{A1})$$

where  $|\psi_k(mT)\rangle = \prod_{n=1}^m U_k(g_n) |\psi_k(0)\rangle$  (the bar above an observable quantity denotes averaging over all disorder configurations) such that the random variable  $g_n$  takes the values 1 and 0 with probabilities (or bias)  $p$  and  $(1-p)$ , respectively, with the following effect:

$$\begin{aligned} U_k(0) &= e^{-iH_0(k)T}, \\ U_k(1) &= e^{-iH_1(k)\frac{T}{2}} e^{-iH_0(k)\frac{T}{2}}. \end{aligned} \quad (\text{A2})$$

In all the instances of explicit symmetry breaking (mentioned in the earlier section) realised in the Hamiltonian  $H_1(k)$ , the configuration averaged stroboscopic particle current and the stroboscopic change in the bulk topological invariant is observed to decay to zero for large stroboscopic intervals of observation [see Figs. 5(a)–5(d) for further details]. We conclude with the note that although we have chosen, a special random protocol in the above discussion,

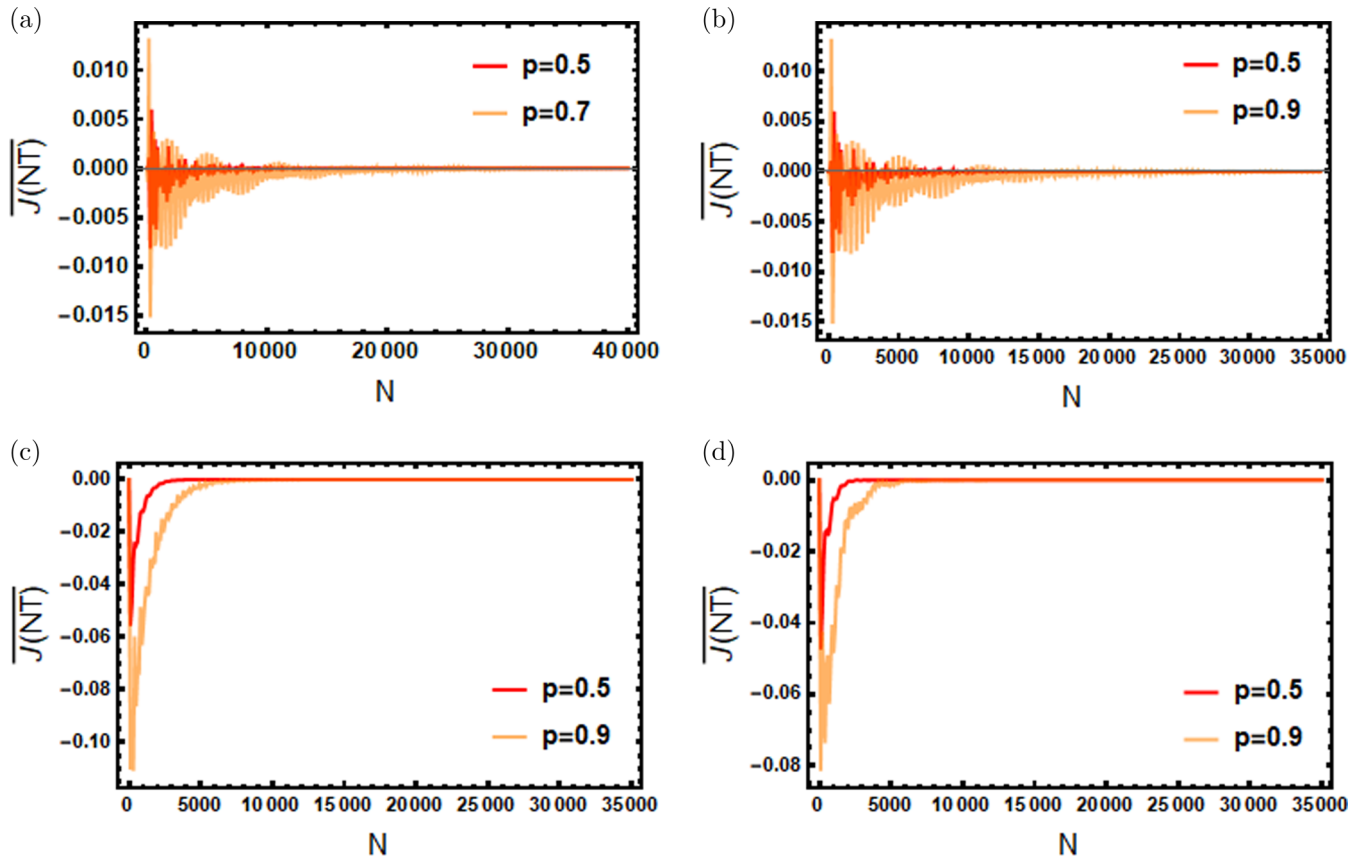


FIG. 5. Disorder averaged stroboscopic particle current in a periodically driven SSH chain in the case of: (a) breaking  $\mathcal{P}$  symmetry by introducing a real NNN hopping in  $H_1(k)$  (as discussed in Sec. IV C) while preserving  $\mathcal{T}$  in  $H_1(k)$ . The initial and final hopping strengths are chosen to be  $v = 2.5$ ,  $w = 1.5$ , and a NNN hopping strength of  $f = 1.0$  for a system size  $L = 500$ ; the frequency of the periodic drive being  $\omega = 100$ . (b) breaking  $\mathcal{P}$  by introducing a staggered mass in  $H_1(k)$  (as discussed in Sec. IV C) while preserving  $\mathcal{T}$  in  $H_1(k)$ . The initial and final hopping strengths are chosen to be  $v = 0.2$ ,  $w = 1.5$ , and a staggered mass of  $M = 1.0$  for a system size  $L = 1000$ , and  $\omega = 100$ . (c) breaking  $\mathcal{P}$  and  $\mathcal{T}$  by introducing an imaginary intercell hopping in  $H_1(k)$  but preserving  $\mathcal{S}$  (as discussed in Sec. IV D). The initial and final hopping strengths are chosen to be  $v = 0.2$ ,  $w = 1.5i$  for a system size  $L = 1000$ , with  $\omega = 100$ . (d) breaking  $\mathcal{P}$ ,  $\mathcal{T}$ , and  $\mathcal{S}$  in  $H_1(k)$  by introducing a staggered mass and an imaginary intercell hopping in  $H_1(k)$  (as discussed in Sec. IV E). The initial and final hopping strengths are chosen to be  $v = 0.2$ ,  $w = 1.5$ , and a staggered mass of  $M = 1.0$  for a system size  $L = 1000$ ,  $\omega = 100$ .

the result obtained is robust and can be shown to hold true for any random perturbation. However, what will happen if one

incorporates dissipation is an interesting question that is not completely settled and a topic of further research.

- 
- [1] A. Kitaev, *Phys.-Usp.* **44**, 131 (2001).  
 [2] C. L. Kane and E. J. Mele, *Phys. Rev. Lett.* **95**, 226801 (2005).  
 [3] B. A. Bernevig, T. L. Hughes, and S.-C. Zhang, *Science* **314**, 1757 (2006).  
 [4] L. Fu and C. L. Kane, *Phys. Rev. Lett.* **100**, 096407 (2008).  
 [5] C. W. Zhang, S. Tewari, R. M. Lutchyn, and S. Das Sarma, *Phys. Rev. Lett.* **101**, 160401 (2008).  
 [6] M. Sato, Y. Takahashi, and S. Fujimoto, *Phys. Rev. Lett.* **103**, 020401 (2009).  
 [7] J. D. Sau, R. M. Lutchyn, S. Tewari, and S. Das Sarma, *Phys. Rev. Lett.* **104**, 040502 (2010).  
 [8] J. D. Sau, S. Tewari, R. M. Lutchyn, T. D. Stanescu, and S. Das Sarma, *Phys. Rev. B* **82**, 214509 (2010).  
 [9] R. M. Lutchyn, J. D. Sau, and S. Das Sarma, *Phys. Rev. Lett.* **105**, 077001 (2010).  
 [10] Y. Oreg, G. Refael, and F. von Oppen, *Phys. Rev. Lett.* **105**, 177002 (2010).  
 [11] A. Kitaev, *Ann. Phys. (N.Y.)* **303**, 2 (2003).  
 [12] A. Kitaev, *Ann. Phys. (N.Y.)* **321**, 2 (2006).  
 [13] F. D. M. Haldane, *Phys. Rev. Lett.* **51**, 605 (1983).  
 [14] M. Levin and X. G. Wen, *Phys. Rev. Lett.* **96**, 110405 (2006).  
 [15] X. G. Wen, *Adv. Phys.* **44**, 405 (1995).  
 [16] V. Mourik, K. Zuo, S. M. Frolov, S. R. Plissard, E. P. A. M. Bakkers, and L. P. Kouwenhoven, *Science* **336**, 1003 (2012).  
 [17] L. P. Rokhinson, X. Liu, and J. K. Furdyna, *Nat. Phys.* **8**, 795 (2012).  
 [18] M. T. Deng, C. L. Yu, G. Y. Huang, M. Larsson, P. Caroff, and H. Q. Xu, *Nano Lett.* **12**, 6414 (2012).  
 [19] A. Das, Y. Ronen, Y. Most, Y. Oreg, M. Heiblum, and H. Shtrikman, *Nat. Phys.* **8**, 887 (2012).

- [20] H. O. H. Churchill, V. Fatemi, K. Grove-Rasmussen, M. T. Deng, P. Caroff, H. Q. Xu, and C. M. Marcus, *Phys. Rev. B* **87**, 241401(R) (2013).
- [21] A. D. K. Finck, D. J. Van Harlingen, P. K. Mohseni, K. Jung, and X. Li, *Phys. Rev. Lett.* **110**, 126406 (2013).
- [22] J. Alicea, *Rep. Prog. Phys.* **75**, 076501 (2012).
- [23] M. Leijnse and K. Flensberg, *Semicond. Sci. Technol.* **27**, 124003 (2012).
- [24] C. W. J. Beenakker, *Annu. Rev. Con. Mat. Phys.* **4**, 113 (2013).
- [25] T. D. Stanescu and S. Tewari, *J. Phys.: Condens. Matter* **25**, 233201 (2013).
- [26] J. E. Moore, *Nature (London)* **464**, 194 (2010).
- [27] S-Q. Shen, *Topological Insulator* (Springer, Berlin, 2012).
- [28] B. A. Bernevig with T. L. Hughes, *Topological Insulators and Topological Superconductors* (Princeton University Press, Princeton, 2013).
- [29] X. G. Wen, *ISRN Condens. Matter Phys.* **2013**, 1 (2013).
- [30] N. R. Cooper, J. Dalibard, and I. B. Spielman, *Rev. Mod. Phys.* **91**, 015005 (2019).
- [31] A. Altland and M. R. Zirnbauer, *Phys. Rev. B* **55**, 1142 (1997).
- [32] L. Fidkowski and A. Kitaev, *Phys. Rev. B* **83**, 075103 (2011).
- [33] M. V. Caspel, S. E. T. Arze, and I. P. Castillo, *SciPost Phys.* **6**, 026 (2019).
- [34] M. Atala, M. Aidelsburger, J. T. Barreiro, D. Abanin, T. Kitagawa, E. Demler, and I. Bloch, *Nat. Phys.* **9**, 795 (2013).
- [35] B. K. Stuhl, H.-I. Lu, L. M. Ayccock, D. Genkina, and I. B. Spielman, *Science* **349**, 1514 (2015).
- [36] G. Jotzu, M. Messer, R. Desbuquois, M. Lebrat, T. Uehlinger, D. Greif, and T. Esslinger, *Nature (London)* **515**, 237 (2014).
- [37] I. Bloch, J. Dalibard, and W. Zwerger, *Rev. Mod. Phys.* **80**, 885 (2008).
- [38] M. Lewenstein, A. Sanpera, and V. Ahufinger, *Ultracold, Atoms in Optical Lattices* (Oxford University Press, Oxford, 2012).
- [39] M. Killi, S. Trotzky, and A. Paramekanti, *Phys. Rev. A* **86**, 063632 (2012).
- [40] P. Hauke, M. Lewenstein, and A. Eckardt, *Phys. Rev. Lett.* **113**, 045303 (2014).
- [41] A. G. Grushin, S. Roy, and M. Haque, *J. Stat. Mech.: Theory Exp.* (2016) 083103.
- [42] T. Kitagawa, E. Berg, M. Rudner, and E. Demler, *Phys. Rev. B* **82**, 235114 (2010).
- [43] N. H. Lindner, G. Refael, and V. Galitski, *Nat. Phys.* **7**, 490 (2011).
- [44] A. Bermudez, D. Patane, L. Amico, and M. A. Martin-Delgado, *Phys. Rev. Lett.* **102**, 135702 (2009).
- [45] A. A. Patel, S. Sharma, and A. Dutta, *Eur. Phys. J. B* **86**, 367 (2013); A. Rajak and A. Dutta, *Phys. Rev. E* **89**, 042125 (2014); P. D. Sacramento, *ibid.* **90**, 032138 (2014).
- [46] M. Thakurathi, A. A. Patel, D. Sen, and A. Dutta, *Phys. Rev. B* **88**, 155133 (2013).
- [47] C. Wang, P. Zhang, X. Chen, J. Yu, and H. Zhai, *Phys. Rev. Lett.* **118**, 185701 (2017).
- [48] M. Tarnowski, F. N. Únal, N. Fläschner, B. S. Rem, A. Eckardt, K. Sengstock, and C. Weitenberg, *Nature Commun.* **10**, 1728 (2019).
- [49] S.-F. Liou and K. Yang, *Phys. Rev. B* **97**, 235144 (2018).
- [50] L. Jiang, T. Kitagawa, J. Alicea, A. R. Akhmerov, D. Pekker, G. Refael, J. I. Cirac, E. Demler, M. D. Lukin, and P. Zoller, *Phys. Rev. Lett.* **106**, 220402 (2011).
- [51] M. Trif and Y. Tserkovnyak, *Phys. Rev. Lett.* **109**, 257002 (2012).
- [52] A. Gomez-Leon and G. Platero, *Phys. Rev. B* **86**, 115318 (2012); *Phys. Rev. Lett.* **110**, 200403 (2013).
- [53] B. Dora, J. Cayssol, F. Simon, and R. Moessner, *Phys. Rev. Lett.* **108**, 056602 (2012).
- [54] J. Cayssol, B. Dora, F. Simon, and R. Moessner, *Phys. Status Solidi RRL* **7**, 101 (2013).
- [55] D. E. Liu, A. Levchenko, and H. U. Baranger, *Phys. Rev. Lett.* **111**, 047002 (2013).
- [56] Q.-J. Tong, J.-H. An, J. Gong, H.-G. Luo, and C. H. Oh, *Phys. Rev. B* **87**, 201109(R) (2013).
- [57] Y. T. Katan and D. Podolsky, *Phys. Rev. Lett.* **110**, 016802 (2013).
- [58] A. Kundu and B. Seradjeh, *Phys. Rev. Lett.* **111**, 136402 (2013).
- [59] V. M. Bastidas, C. Emary, G. Schaller, A. Gómez-León, G. Platero, and T. Brandes, *arXiv:1302.0781v2*.
- [60] T. L. Schmidt, A. Nunnenkamp, and C. Bruder, *New J. Phys.* **15**, 025043 (2013).
- [61] A. A. Reynoso and D. Frustaglia, *Phys. Rev. B* **87**, 115420 (2013).
- [62] P. M. Perez-Piskunow, G. Usaj, C. A. Balseiro, and L. E. F. Foa Torres, *Phys. Rev. B* **89**, 121401(R) (2014).
- [63] B. Mukherjee, A. Sen, D. Sen, and K. Sengupta, *Phys. Rev. B* **94**, 155122 (2016).
- [64] A. Sen, S. Nandy, and K. Sengupta, *Phys. Rev. B* **94**, 214301 (2016).
- [65] T. Oka and H. Aoki, *Phys. Rev. B* **79**, 081406(R) (2009).
- [66] T. Kitagawa, T. Oka, A. Brataas, L. Fu, and E. Demler, *Phys. Rev. B* **84**, 235108 (2011).
- [67] M. S. Rudner, N. H. Lindner, E. Berg, and M. Levin, *Phys. Rev. X* **3**, 031005 (2013).
- [68] L. E. F. Foa Torres, P. M. Perez-Piskunow, C. A. Balseiro, and G. Usaj, *Phys. Rev. Lett.* **113**, 266801 (2014).
- [69] H. Dehghani, T. Oka, and A. Mitra, *Phys. Rev. B* **91**, 155422 (2015).
- [70] J. H. Wilson, J. C. W. Song, and G. Refael, *Phys. Rev. Lett.* **117**, 235302 (2016).
- [71] L. D'Alessio and M. Rigol, *Nature Commun.* **6**, 8336 (2015).
- [72] M. D. Caio, N. R. Cooper, and M. J. Bhaseen, *Phys. Rev. Lett.* **115**, 236403 (2015).
- [73] U. Bhattacharya, J. Hutchinson, and A. Dutta, *Phys. Rev. B* **95**, 144304 (2017).
- [74] S. Mardanya, U. Bhattacharya, A. Agarwal, and A. Dutta, *Phys. Rev. B* **97**, 115443 (2018).
- [75] M. McGinley and N. R. Cooper, *Phys. Rev. Lett.* **121**, 090401 (2018).
- [76] Z. Gong and M. Ueda, *Phys. Rev. Lett.* **121**, 250601 (2018).
- [77] N. Flaschner, D. Vogel, M. Tarnowski, B. S. Rem, D. S. Luhmann, M. Heyl, J. C. Budich, L. Mathey, K. Sengstock, and C. Weitenberg, *Nat. Phys.* **14**, 265 (2018).
- [78] C. Yang, L. Li, and S. Chen, *Phys. Rev. B* **97**, 060304(R) (2018).
- [79] M. McGinley and N. R. Cooper, *Phys. Rev. B* **99**, 075148 (2019).
- [80] M. D. Caio, G. Möller, N. R. Cooper, and M. J. Bhaseen, *Nat. Phys.* **15**, 257 (2019).

- [81] M. S. Foster, M. Dzero, V. Gurarie, and E. A. Yuzbashyan, *Phys. Rev. B* **88**, 104511 (2013).
- [82] M. S. Foster, V. Gurarie, M. Dzero, and E. A. Yuzbashyan, *Phys. Rev. Lett.* **113**, 076403 (2014).
- [83] A. Russomanno, A. Silva, and G. E. Santoro, *Phys. Rev. Lett.* **109**, 257201 (2012).
- [84] X. Zotos, F. Naef, and P. Prelovsek, *Phys. Rev. B* **55**, 11029 (1997).
- [85] T. Kitagawa, M. S. Rudner, E. Berg, and E. Demler, *Phys. Rev. A* **82**, 033429 (2010).
- [86] J. K. Asbóth, *Phys. Rev. B* **86**, 195414 (2012).
- [87] J. K. Asbóth and H. Obuse, *Phys. Rev. B* **88**, 121406(R) (2013).
- [88] S. Nandy, A. Sen, and D. Sen, *Phys. Rev. X* **7**, 031034 (2017).
- [89] U. Bhattacharya, S. Maity, U. Banik, and A. Dutta, *Phys. Rev. B* **97**, 184308 (2018).
- [90] S. Maity, U. Bhattacharya, and A. Dutta, *Phys. Rev. B* **98**, 064305 (2018).